LRS2: a new low-resolution spectrograph for the Hobby-Eberly Telescope*

Hanshin Lee[a,†], Taylor S. Chonis[b], Gary J. Hill[a], Darren L. DePoy[c], Jennifer L. Marshall[c], Brian Vattiat[a]

[a] McDonald Observatory, University of Texas at Austin, 1 University Station C1402, Austin, TX 78712-0259, USA

[b] Department of Astronomy, University of Texas at Austin, 1 University Station C1401, Austin, TX 78712-0259, USA

[c] Department of Physics and Astronomy, Texas A&M University, 4242 TAMU, College Station, TX 77843-4242, USA

ABSTRACT

In the era of the Hobby-Eberly Telescope (HET) Wide-Field Upgrade (WFU), the current Low-Resolution Spectrograph (LRS) will be replaced with a more capable red-optimized fiber instrument, called LRS2. This new spectrograph will be based on the Visible Integral-field Replicable Unit Spectrograph (VIRUS) that was designed to be easily adapted to a wide range of spectral resolutions, and wavelength ranges. The current snapshot of LRS2, fed by a 7x12 sq. arcsec fiber integral-field unit (IFU), covers 350-1100 nm, simultaneously at a fixed resolving power R~1800, with the wavelength range split into two pairs of spectrographs, one for the blue to red wavelength range (350-630 nm) and the other for the red and far-red range (630-1100 nm). These units are designated LRS2-B and LRS2-R, respectively. Only minimal modification from the base VIRUS design in gratings (for both pairs) and in the detector (for the red pair only) is required. In addition to this flexibility, the generic nature and massively replicable characteristic of the instrument can allow us to adapt the instrument to a wide range of not only telescope diameters (1 m ~ 40 m), but also observing modes (single to multiple objects). We discuss the current snapshot of the LRS2 design.

Keywords: Low-resolution spectrograph, Hobby-Eberly Telescope, VIRUS

1. INTRODUCTION

In the next two years, the 10 m Hobby-Eberly Telescope (HET) will be upgraded to have a much larger field of view (22 arcmin.) and improved performance[1]. We will outfit the HET with VIRUS, which will consist of 75 copies of a simple unit spectrograph pair, fed by 33,600 optical fibers[2]. The current Marcario Low Resolution Spectrograph (LRS) was the first facility instrument delivered and has been the workhorse instrument on the HET for the past decade[3]. The LRS must now be replaced since the design is not compatible with the Wide Field Upgrade (WFU), and we need improved efficiency, particularly in the red to remain competitive.

The LRS2 design is based on the VIRUS unit spectrograph that was designed to be adaptable to a wide range of spectral resolutions, and wavelength ranges. LRS2 will be the first demonstration of such an application, and will be fed by a 7x12 sq. arcsec fiber integral-field unit (IFU) and cover 350-1100 nm, simultaneously at a fixed resolving power R~1800. Two unit pairs will consist of the LRS2, one optimized to cover the blue to red wavelength range (350 – 630 nm) and the other to cover the red to far red wavelength range (630 – 1100 nm). The blue-optimized pair (LRS2-B) will be a straight adaptation of the VIRUS unit, employing the same CCD detectors. The only difference will be modified gratings. The red-optimized pair (LRS2-R) will employ Lawrence Berkeley National Laboratory's fully depleted thick CCD detectors (LBNL hereafter) that offer much higher efficiency and no fringing at long wavelengths, greatly improving performance over the current LRS.

---

* The Hobby – Eberly Telescope is operated by McDonald Observatory on behalf of the University of Texas at Austin, the Pennsylvania State University, Stanford University, Ludwig-Maximillians-Universität München,and Georg-August-Universität, Göttingen

† Hanshin Lee.: E-mail: lee@astro.as.utexas.edu

Ground-based and Airborne Instrumentation for Astronomy III, edited by Ian S. McLean, Suzanne K. Ramsay, Hideki Takami, Proc. of SPIE Vol. 7735, 77357H · © 2010 SPIE · CCC code: 0277-786X/10/$18 · doi: 10.1117/12.857201

LRS2 is being designed at the University of Texas at Austin (UT) and assembled at the Texas A&M University (TAMU). Penn State University (PSU) will lead the commissioning. We expect to deploy LRS2-B in mid 2011 with the HET WFU, ensuring the continuity of capable low-resolution spectroscopy on HET. Utilizing the VIRUS unit as the basis for LRS2 allows us to leverage the large engineering investment in the VIRUS development to greatly reduce the cost and speed the delivery, since only limited new engineering is required and LRS2 can be built on the production line for VIRUS at TAMU[38]. The large separate investment in VIRUS also makes the budget relatively low for such a capable instrument.

The LRS2 is designed to exploit the strengths of the queue-scheduled HET in surveys and synoptic observations, and will offer rapid set-up, high efficiency, and great stability. We will apply LRS2 to spectroscopy on large samples of faint objects selected from upcoming large surveys such as HETDEX and DES, synoptic observations to provide time-resolved data on variable phenomena such as AGN, and targets of opportunity such as supernova explosions and γ-ray bursts. In addition to this flexibility, the generic nature and massively replicable characteristic of the instrument can allow us to adapt the instrument to a wide range of not only telescope diameters (1m ~ 40m), but also observing modes (single to multiple objects). We discuss the current LRS2 design and its implication in the era of the future Extremely Large Telescopes (ELT).

2. LRS2 SCIENCE

Demand for LRS2 can be predicted based on usage and impact of LRS. Its versatility is well suited to time-critical synoptic and target of opportunity (ToO) observations and to large area surveys to classify faint objects. While there is not space to document a decade of science, we present short summaries of representative areas where current work with LRS will be extended or enhanced by LRS2.

Transient Phenomena - Supernovae (SNe) and Gamma Ray Bursts (GRBs): The responsive queue scheduling of HET coupled with the broad wavelength coverage of the current LRS in its lowest resolution mode have proven very powerful in responding to transient events such as SNe and GRBs. A prime example is the recently completed SDSS–II Supernova Survey[4-5] which benefitted from the combined survey and synoptic strengths of the telescope. HET provided spectra of the most distant third of the sample, ~200 objects, with a median redshift of z~0.3, extending to z=0.5. HET was the primary telescope used for the highest redshift supernovae in the survey. The typical brightness of the targets was r=21.5 (faintest at r=22.5), all observed with two 1200 s exposures. The responsive queue of the HET allowed the majority to be observed within 24 hours of discovery. This project was ideally suited to the HET since SDSS-II targeted a long constant-declination strip, and the queue was able to follow up new targets, rapidly. HET LRS has obtained rapid response spectra of about a dozen GRBs[6-8], including the brightest ever observed[9]. While the telescope can only access a limited range of hour angle at any moment, the rapid responses of the queue and its position on the Earth have enabled the HET to be quite competitive in this area. PSU operates the SWIFT satellite that has revolutionized the study of GRBs by providing more accurate coordinates from X-ray observations. GRBs have now been discovered out to z~8, and the wide wavelength coverage of LRS2, particularly the high red efficiency, will make it an ideal instrument for these studies. Such GRBs will provide many lines of sight through the high redshift IGM, probing reionization. One of the key issues in this research is the ability to rapidly acquire the object, often based on coordinates with errors much larger than an arcsecond. The integral field of LRS2 will not require precise coordinates, reducing overhead considerably on these time-critical observations. The IFU will also improve 2-D background subtraction of the underlying host galaxies of SNe and GRBs.

Survey Follow-up: LRS2 on HET will play a uniquely important role as a follow-up instrument for interesting objects in large surveys, given its wide wavelength coverage, excellent sky subtraction, and ability to observe efficiently in survey mode. Huge planned imaging surveys (Dark Energy Survey, Pan-Starrs, LSST) will search for many types of object, including near-Earth asteroids and comets in the outer solar system, the coldest and nearest brown dwarfs, stars in the halo of our Galaxy, galaxy clusters, and QSOs and galaxies in the distant universe. To verify the nature of these sources and to study them in detail, follow-up spectroscopy will be essential. Many of the objects will be brighter at redder wavelengths. The combination of the exceptional red sensitivity of LRS2 and the queue scheduling of HET will make LRS2 ideally suited for their follow-up spectroscopy. HETDEX, which starts observations at the end of 2011, will conduct a blind spectroscopic survey covering 420 sq. deg in the northern galactic cap, detecting a million Ly-α emitters (LAEs) from $1.9<z<3.5$ and a million [OII] emitters at $z<0.5$, as well as large numbers of QSOs, AGN, stars, clusters of

galaxies etc. down to the sensitivity limit SDSS imaging survey. This unique dataset will require follow-up with LRS2 to establish the classification of emission-line objects (LAE, [OII], AGN), to classify extremely metal poor stars, to study emission-line diagnostics over a wider wavelength range, for example. In particular, given the large sample from HETDEX, LRS2 is the ideal instrument to follow-up the most interesting LAEs (e.g., largest mass, highest star formation rate, highest specific stat formation rate, etc.) at the epoch when the star formation rate was peaking and most galaxy assembly occurred. Obtaining higher resolution spectra and large wavelength coverage will allow the Ly-α line profiles and other emission lines (e.g. CIV) to be studied, probing the ISM in these galaxies. Ly-α blobs with sizes as large as 100 kpc will be found in unprecedented numbers in HETDEX and can also be studied in great detail with the IFU of LRS2. These objects may be sites of intense in-fall of gas (as recently observed by Adams et al. 2009 using the VIRUS prototype[10]) or strong wind outflows. Understanding galactic winds is another field ripe for advancement over the next decade, and HETDEX will provide a huge sample of blue compact dwarf galaxies at $z<0.5$ where LRS2 can search for the emission-line diagnostics of outflows.

High Redshift Quasars and Other AGN: The large area photometric surveys needed to identify high redshift QSO candidates are ideally suited to spectroscopic follow-up in survey mode with HET. HET has made important contributions to identifying candidates from the SDSS and CFHT Legacy surveys[11-13]. With UV and far-red sensitivity, LRS2 will be superb for spectroscopic follow up of a wide range of imaging surveys from X-ray to infrared and radio wavelengths[14-16]The short setup time will also make such surveys significantly more efficient than with the current LRS. A particularly powerful feature of LRS2 is that the spectral resolution is fixed and the IFU adapts the data to any image quality without losing light at the entrance aperture. Calibrations will also be simple and stable.

Brown Dwarfs: Spectroscopy in the red (0.6-1.0 μm) is a vital tool for identifying and studying brown dwarfs. The spectral types of M and L dwarfs are defined by molecular absorption bands in the far red (TiO, VO[17,18]), and Hα emission is a diagnostic of accretion from circumstellar disks[19,20], while gravity-sensitive atomic absorption lines (K I, Na I) provide constraints on ages of brown dwarfs[21]. Red optical spectroscopy is particularly powerful for confirming brown dwarf candidates that are identified in photometric surveys of young clusters in star-forming regions because brown dwarfs are relatively warm and bright at optical wavelengths when they are young. As an example, the current LRS on HET has been used to confirm brown dwarf candidates in Taurus down to 15 M_{Jup} (<M9, I<20[22-25]). By employing more sensitive optical spectrometers at Gemini Observatory, this work has been extended to even lower masses, discovering a few brown dwarfs down to ~5 M_{Jup} in Taurus and 4 Chamaeleon (L0, I<22[24,25]). These results are important for measuring the minimum mass at which star-like objects can form, providing a fundamental test of theories of star and planet formation. The sensitivity of LRS2 at red optical wavelengths will be comparable to that of Gemini, allowing us to use HET for much larger surveys for planetary mass brown dwarfs in star-forming regions than we can currently perform with Gemini alone.

3. CURRENT SNAPSHOT OF LRS2 INSTRUMENTATION

LRS2 is based on the unit spectrograph developed for VIRUS and benefits greatly from the large investment made in the design, prototyping, and production line engineering. Modifications to the unit spectrograph for LRS2 are minor, allowing us to speed the deployment of LRS2 to coincide with the installation of the HET WFU in mid 2011. We describe the key design features of VIRUS and then the adaptation of the unit spectrograph to LRS2.

3.1 Description of VIRUS as a Building Block for LRS2

VIRUS is optimized to be fed by fibers, illuminated at f/3.65. The optical design (Fig. 1) consists of a reverse-Schmidt collimator and a Schmidt camera, with a shared corrector plate, utilizing volume phase holographic (VPH) gratings for dispersion. The focal reduction factor is 2.8. While intended for the UV-green region of the spectrum, the design is highly pan-chromatic since all the power is in the two spherical mirrors, which can be supplied with different coatings to optimize the instrument for different band passes. The design images superbly, and the dispersion and wavelength range can be further adapted using grisms which can be readily exchanged in the mechanical design. VIRUS is designed to be fed by a simple "densepak" type IFU (Fig. 2), where the fibers are arrayed in a hexagonal close-pack with exactly 1/3 fill-factor at the input, fed directly at f/3.65 by the WFC. An observation with VIRUS consists of three exposures with small offsets (dithers of ~1 arcsec.), to fill in the sky coverage gaps between the fibers of the IFUs. The dithers are achieved by moving the focal plane assembly that mounts the IFUs and is independent of guiding in order to guarantee very precise knowledge of the relative positions of the three exposures that make up an observation.

We have constructed a prototype, VIRUS-P[26], which has been used on the McDonald 2.7 m for the past two years to verify the performance of the instrument and to undertake a pilot survey of emission-line galaxies in support of HETDEX. VIRUS-P has demonstrated the high throughput, excellent image quality, very low ghosting, and exceptional stability of the design, which has been evolved into the final replicated units for production[27]. VIRUS-P has proven to be a powerful instrument in its own right, with applications from high redshift galaxies[10], to nearby galaxies, to 6 planetary nebulae[28]. In production, each VIRUS unit has a pair of spectrographs in a common housing, reducing costs, and two of these unit pairs will form the basis of LRS2.

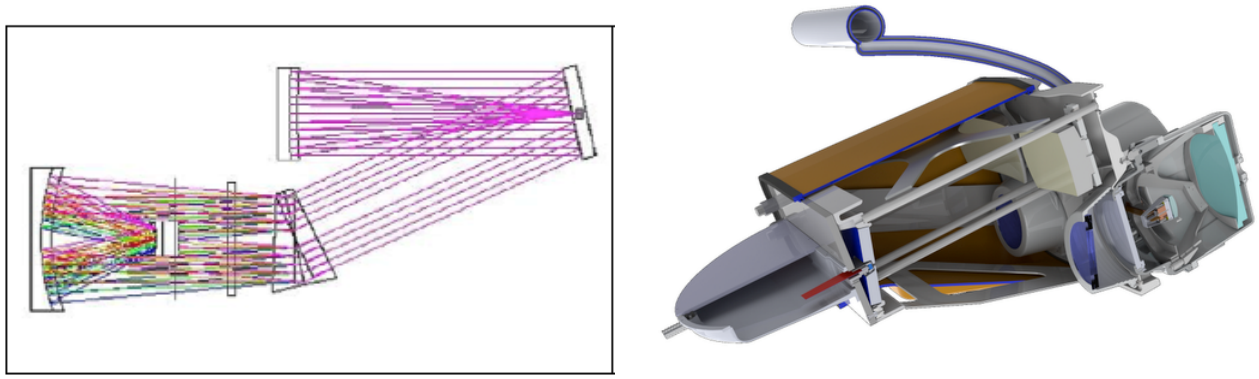

Figure 1: Optical and Mechanical Layout of LRS2. Left is the optical design of the Red spectrograph. The fiber "slit" is orientated out of the page. For scale, the beamsize is 115 mm. The only change from VIRUS is the grism disperser. The other 3 spectrographs are the same, except for small differences in the grisms. Right shows the mechanical design of the VIRUS unit on which LRS2 is based, incorporating a pair of the spectrographs. The format is fixed and there are no moving parts. The structure is all Aluminum, except for invar struts that maintain focus. The fiber IFU "slits" mount to the bulkhead on the right.

3.2 Basic Description of LRS2

The VIRUS unit spectrograph is designed to be adaptable to a wide range of telescopes, spectral resolutions, and wavelength ranges. LRS2 will be the first demonstration of such an application, and will consist of two unit pairs, LRS2-B (350 – 650 nm) and LRS2-R (650 – 1100 nm). Fig. 1 shows the optical design of one of the four spectrographs (left panel) along with the mechanical design of the VIRUS unit spectrograph on which LRS2 is based (right panel). Replacement of the grating in VIRUS with grism dispersers and customization of the optical coatings are the main adaptation needed to utilize the VIRUS design for LRS2. LRS2 will utilize lenslet-coupled fiber integral field units (IFU) with 170 μm core diameter fiber, fed simultaneously via a focal expander with dichroic beamsplitters to divide the spectrum among the four spectrographs (Fig. 3). Table 1 presents the proposed wavelength ranges and resolving powers of each of the four spectrographs that make up LRS2, along with VIRUS and the current LRS for comparison.

Table 1. Wavelength coverage of the LRS2 spectrograph, VIRUS, and LRS.

Unit ID		λ_{MIN} [nm]	λ_{MAX} [nm]	R	CCD	Grating [$^{line}/_{mm}$]	Prism angle [degree]
LRS2	Blue	350	470	1821	VIRUS	1090	6.0
	Green	465	625	1815	VIRUS	810	6.0
	Red	620	835	1803	LBNL	890	14.0
	Far-red	830	1100	1904	LBNL	740	16.7
VIRUS		350	550	700	VIRUS	930	None
LRS		430	1000	300-1500	Loral	varies	varies

The exact wavelengths of the splits are being decided in consultation with HET users, since there is inevitable loss of S/N ratio around the wavelengths of the splits, and we wish to minimize the science impact. The blue-optimized pair (LRS2-B) will be a straight adaptation of the VIRUS unit, employing the same CCD detectors, and will be assembled

on the VIRUS production line requiring little new engineering. The only difference will be that the VPH gratings will be optimized for the wavelength range of each spectrograph, and will be immersed between BK7 prisms to form grisms. The red-optimized pair (LRS2-R) will employ thick, fully-depleted CCD detectors developed by LBNL for the Dark Energy Survey[29] that have much higher efficiency at long wavelengths and will require some additional engineering to adapt the VIRUS design for their use. Experience with VIRUS-P and detailed Monte Carlo modeling of the optical tolerances for VIRUS in production, including the modulation transfer function of the detectors and charge diffusion in the thick LBNL chips, indicates that the variation in the full-width half-maximum of the point spread functions of the spectrographs can be kept to 1.0 pixel or better, convolved with the image of the fiber core. For 170 μm core fiber, this yields the resolving powers in Table 2, for 1-D extracted spectra. Fiber separation on the detector is set to minimize cross-talk between overlapping spectra, which sets the number of fibers and the field of view of the IFU (Table 2).

Table 2. IFU input parameters.

Focal ratio	Lenslet pitch		Mircro pupil size [mm]	Fiber diameter [mm]	# of lenslets	Field diameter [arcsec]	Alternative format
	[mm]	[arcsec]					
f/11	0.35	0.62	0.16	0.17	287	10.5	7”×12”

The resolving power of R~1800 is chosen due to science drivers such as splitting the [OII]3727 doublet, and to ensure good sky subtraction in the far red where the strong OH bands dominate the sky. It is desirable to have approximately constant R over the full wavelength range to allow diagnostic spectral features to be analyzed at the same resolution over the whole wavelength range. Similarly, matching the lenslet spatial elements (spaxels) on the sky between the four spectrographs is desirable if extended objects are being analyzed, and this registration can be done to 0.05 arcsec (30 μm). In the UV, LRS2 data will be read-noise dominated in normal exposure times (Table 4), but VIRUS is the better instrument to survey very faint objects in the UV and the different spectral resolutions of LRS2 and VIRUS make them highly complementary: LRS2 will be used to follow up objects found by VIRUS.

3.3 Integral Field Unit and Input Optics

Figure 2: VIRUS IFU Construction. The left panel shows a slit for a single spectrograph in a production jig. The middle panel shows the double slit end of a production IFU prior to integration into its housing. The right panel shows how the input ends of the IFUs for VIRUS (only a few shown) and the feed for LRS2 at the center of the field will be integrated together to allow parallel observing. The inset shows the input end of the VIRUS-P IFU.

For LRS2 we desire IFUs with close to 100% fill-factor, and sufficient field area to make acquisition easy and to guarantee adequate sky in all image quality conditions. The proven way to meet this requirement is by coupling the image plane to the fibers by way of a microlens array, which forms micro-pupil images on the fiber ends[30]. This lenslet-coupling is particularly effective for the HET as the azimuthal scrambling provided by the fibers ensures an extremely stable output beam into the spectrographs independent of the illumination factor of the HET pupil, which changes as HET tracks. The one drawback is that the pupil formed within the spectrograph no longer exhibits the central obstruction of the telescope, so light losses are higher than in the case of imaging directly onto the fibers as in VIRUS. Modern lenslet arrays fabricated from fused silica are of very high quality, and we have demonstrated the ability to create fiber bundles with an input matrix accurate to <5 μm p-p in the VIRUS IFUs[31], so excellent coupling to the fibers can be guaranteed. In addition we have designed the input optics and lenslets to underfill the fiber core with the micropupil images, minimizing light loss, though at the expense of a little lost spectral resolution (since the output

image will be the diameter of the fiber core, which is larger than the input micropupil diameter. The input into the fiber is f/3.5 (VIRUS accepts f/3.4, so a small amount of focal ratio degradation and misalignment is allowed for). Table 2 presents the parameters of the input optics and microlens array.

The additional requirement on the feed design is that it fit within space available at the center of the field of view of the upgraded HET. Fig. 2 (far right) illustrates the space available within the layout of IFUs for VIRUS, taking up the central four slots, and shows how the LRS2 feed integrates with the VIRUS IFU cables. Space is limited, but this configuration allows the LRS2 fiber cables to follow the same route as those for VIRUS and enables a parallel observing mode where VIRUS gathers data of the surrounding field any time LRS (or other HET instruments) are used. This mode is very powerful for increasing the size of samples of objects from VIRUS, and is strongly desired by the HET community. The one drawback for LRS2 is that the dithering required to fill in the areas of the VIRUS IFUs will cause (one arcsec.-level) offsets of the image at the LRS2 input, but these offsets can be coordinated with the readout of LRS2 as well as VIRUS and will aid in providing three independent exposures within each LRS2 observation. In designing the input optics, the small available space has been taken into account, but does not become a limiting factor. The spectrographs can accommodate 287 fibers with appropriate gaps, covering a 10.5 arcsec diameter field. The input optics can accept a 14 arcsec. diameter, so an alternative format that provides sky coverage further from the object is 7" x 12". The elongated field has desirable properties, but the final configuration will be determined in the preliminary design phase.

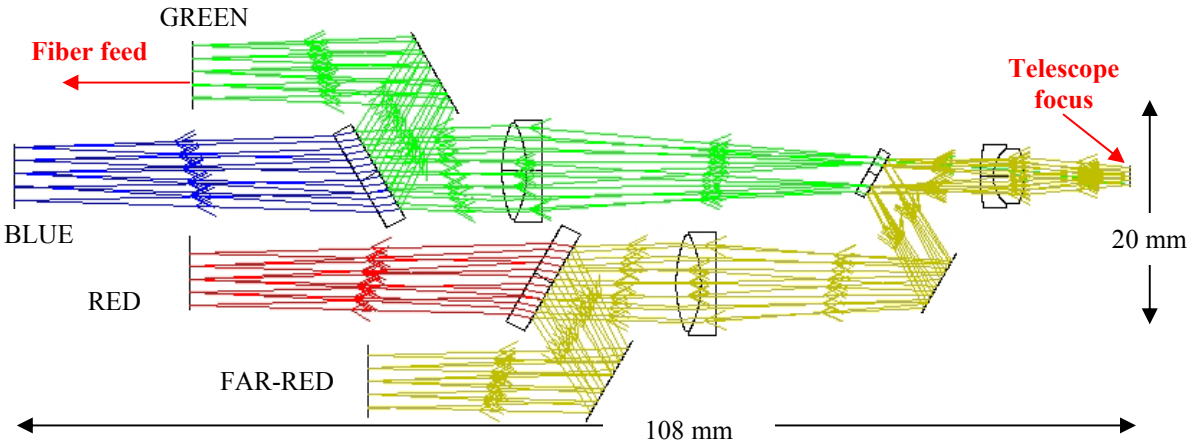

Figure 3: Optical Design of the IFU Feed for LRS2**.** Light from the input field is collimated and split into four wavelength ranges by a series of 3 dichroics. Each wavelength range is focused onto a lenslet - coupled fiber array and is transmitted to a separate spectrograph. The design is "folded-out" for clarity.

The input optics (Fig. 3, Table 2) include three dichroic beamsplitters to divide the light in wavelength between the four spectrographs. Broad-band light from the input aperture is collimated, split, and then reimaged at f/11 onto the lenslet arrays at the input to each of the IFUs. The fiber bundle from each IFU is routed to a single spectrograph within LRS2. Experience with dichroics indicates that the design of the multi-layer coatings will be straight-forward, but care must be exercised in choice of the angle of incidence and substrate thickness. Low angles of incidence yield a design with a sharper transition in wavelength between reflection and transmission, so the optics have been designed for 30 degrees incidence angle, rather than 45 degrees as is common. Surface tension effects, due the different CTE of the multi-layer coating on one side of the substrate, can warp the substrate putting power into the reflected beam. This is not a great effect if the curvature is measured and compensated with each camera lens, but we have adopted a 6:1 ratio of diameter to thickness to minimize this setup adjustment. The design is still preliminary, using Fused Silica and LLF1 for the optics, but produces excellent images at all wavelengths and will fit in the space available in the focal surface assembly. It will be completed and toleranced during the design phase for LRS2. Coupling into the fibers is better than 90%, including diffraction and fiber centering effects.

3.4 Cameras and Detector Systems

The LRS2-B pair will utilize UV-blue optimized thinned 2064x2064 CCDs with 15 μm pixels, identical to those of

VIRUS, while the LRS2-R pair will use fully-depleted LBNL CCDs with the same format, developed for the DECam project [29]. The VIRUS detector system is being supplied by Astronomical Research Cameras Inc [2]. The requirements for LRS2-B are identical to those for VIRUS: high QE in the UV/blue, read noise of 3.5 electrons or better, and readout time of 20 seconds binned 2x1. Since we are purchasing 150-200 systems (detectors plus controllers) for VIRUS, we can add the CCDs and controllers to the order without difficulty, and may be able to select particularly good detectors for LRS2-B. The LBNL CCDs for LRS2-R require large negative bias voltages, which are not within the required capabilities of the controllers for VIRUS. These detectors have demonstrated read noise of 3.5 electrons at 50 kpxl/s in tests at Fermilab [29]. All LRS2 detectors to be read out by the same data system architecture as VIRUS. LRS2 CCDs will be read out through a dedicated data acquisition computer, rather than through the VIRUS detector system multiplexed readout, since we will operate the instruments independently, but they do share the shutter with VIRUS so the data systems must coordinate.

The other new development needed to utilize the LBNL CCDs is to redesign the detector head to mount the CCDs, which have a different package design to those optimized for VIRUS. Fortunately, the LBNL CCDs are fully 4-edge abuttable, and hence can fit within the same tight envelope as the VIRUS CCDs. By adapting the VIRUS detector system for LRS2, we make use of the design and investment in the cryostats and cryogenic and readout infrastructure for VIRUS. VIRUS will have a simple, though extensive, LN2 distribution system that will be fed from header tanks that are replenished from a large external dewar. The dewar will be refilled by tanker every two weeks. Each pair of spectrographs will have a "dogleg" of vacuum jacketed flexible hose terminating in a copper heat exchanger bayonet that will conduct heat out of the VIRUS/LRS2 camera cryostat, yet allow the camera to be disconnected with ease from the cryogen system[32]. The design of the novel bayonet has been tested with a prototype and demonstrated to meet design requirements. In particular, if the bayonet is disconnected and inverted a nitrogen gas bubble vapor lock is generated and conductivity is shut down, allowing that camera to be safely removed without affecting the rest of the system. We intend to outfit the LRS2 cryostats and spares with full range vacuum gauges, higher quality vacuum fittings, and ion pumps so as to ensure better longevity of their vacuums. We are currently undertaking cryogenic tests to see the effect of periodic warm up and re-pumping to maintaining the vacuum. This is acceptable for VIRUS since we do not require all spectrographs to be on-line, but for LRS2 we wish to avoid downtime, and experience with the current LRS indicates that we will maintain the vacuum for periods well in excess of 18 months so long as the instrument remains cold.

3.5 Predicted Performance of LRS2

We can predict the performance of LRS2 very well, based on the VIRUS-P prototype that has been in use since October 2006. The design and performance of VIRUS-P is described[26]. The optical performance of VIRUS-P meets specifications for HETDEX, and detailed Monte-Carlo simulation of the production VIRUS optics indicates that (statistically) manufacturing, mounting, and alignment tolerances will result a 1.0 pixels variation in the FWHM point spread function, for any collimator and camera pair so that the parts are fully interchangeable[33]. Since LRS2 is a special case, and we do not require interchangeability, we will expend considerably more effort on its alignment than on a typical VIRUS spectrograph, and fully expect to meet the image quality requirements for the higher resolution required of LRS2. Indeed we have already done so with VIRUS-P.

Improvements in sensitivity over the current LRS are primarily in the red parts of the spectrum, where the optimized CCD detectors provide several times greater sensitivity, and no fringing. LRS2-B also extends coverage down to the UV. We have modeled the throughput of LRS2 based on the same model used for VIRUS with an additional factor of 0.9 applied to account for the use of lenslets and including the effect of the obstruction of the detector. We have included diffraction effects in the simulation of coupling to the IFU, but they are small (<5%) for all wavelengths. This model has been verified against on-sky measurements with VIRUS-P[26] and demonstrated to be accurate to better than 10%, so we feel confident in making an extrapolation from it. Fig. 4 shows the throughput for each of the spectrographs as a function of wavelength. The throughput of the upgraded HET is expected to be 65% at 600 nm, with a minimum requirement of 50%, including obstructions. There are no aperture slit losses, as with a slit spectrograph, due to the integral field feed of LRS2.

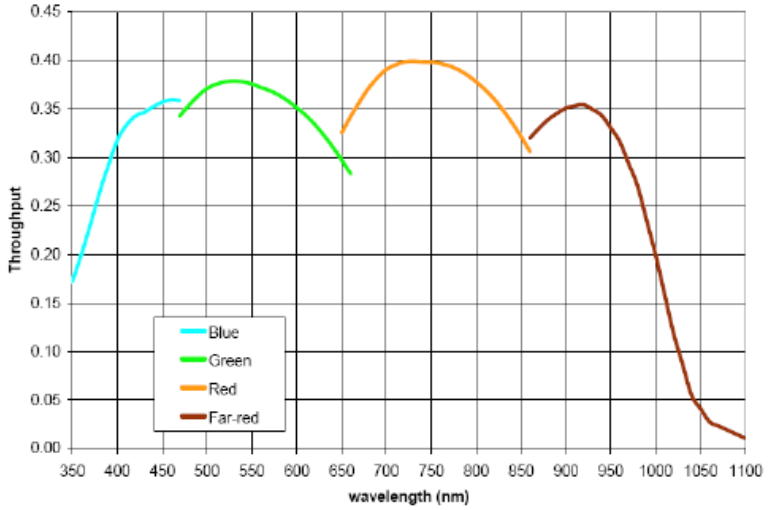

Figure 4. Predicted throughput of LRS2 including the IFU and spectrograph, but excluding the HET and atmosphere. The same model has been verified on sky for VIRUS-P. The exact edges of the dichroic beamsplitter bandpasses have not been included, but they will be designed to have sharp transitions at wavelengths close to 470, 620, & 830 nm.

Table 3. Performance measures for LRS2.

Wavelength [nm]	350	450	500	600	750	950
Limiting AB magnitude in 30min (5-sigma / resolution element)	22.6	23.3	23.7	23.4	23.6	22.6
Minimum exposure (sec) for sky noise > read noise	5300	1830	890	560	650	600

The LRS2 team has already developed software packages that can simulate both 1D and 2D LRS2 data; the latter will be particularly important for development of the LRS2 analysis code prior to any on sky observations. These simulated images can already be processed using the packages developed for VIRUS-P, so the incremental effort required to tailor the software to LRS2 is not excessive. Based on these models, we have simulated representative observations to predict performance. Table 4 summarizes the sensitivities and indicates the exposure time needed for a single resolution element (binned 2x1) to become sky noise dominated for the continuum.

3.6 Operation of LRS2

A key operational aspect of LRS2 over the current LRS is the change to an Integral Field Unit fiber feed (IFU) from a slit for the entrance aperture of the instrument. The IFU should reduce the target acquisition time significantly to about a minute from the current value of approximately 10 minutes, when coupled with the improved metrology provided by the WFU. LRS2 is also designed to operate in parallel with the VIRUS instrument, so that VIRUS will be gathering data in the surrounding field at the same time as LRS2 is observing an object. This capability is enabled by the design of the IFU for LRS2 and is seen as a major benefit for the science output of the telescope. Software has been developed for VIRUS-P and has demonstrated Poisson-noise dominated sky subtraction over the 350-585 nm range over hundreds of nights of observation on the McDonald 2.7 m. Tests extending to 670 nm have also demonstrated sky-noise-limited subtraction. The instrument is extremely stable, exhibiting only a very small “breathing” of the image at the 0.1 pixel level (1/20 of the resolution element) with temperature changes of 5 Celsius. The instrument is rack mounted, so gravity invariant. We expect VIRUS to be even more stable due to improvements to the camera design.

4. SUMMARY

In the grand view of future instrument development in astronomy, LRS2 will demonstrate the adaptation of the VIRUS unit spectrograph to be a powerful broadband low-resolution instrument on a large telescope. The same design will also be well adapted to future applications on the next generation of 20-40 m class telescopes, and offers an extremely cost-effective way to instrument such telescopes.

ACKNOWLEDGEMENTS

HETDEX is led by the University of Texas at Austin with participation from the Universitäts-Sternwarte of the Ludwig-Maximilians-Universität München, the Max-Planck-Institut für Extraterrestrische-Physik (MPE), Astrophysikalisches Institut Potsdam (AIP), Texas A&M University, Pennsylvania State University, and the HET consortium. HETDEX is funded in part by gifts from Harold C. Simmons, Robert and Annie Graham, The Cynthia and George Mitchell Foundation, Louis and Julia Beecherl, Jim and Charlotte Finley, Bill and Bettye Nowlin, Robert and Fallon Vaughn, Eric Stumberg, and many others, by AFRL under agreement number FA9451-04-2-0355, and by the Texas Norman Hackerman Advanced Research Program under grants 003658-0005-2006 and 003658-0295-2007.

REFERENCES

[1] R. Savage, et al., "Current Status of the Hobby-Eberly Telescope wide field upgrade," Proc. SPIE, **7733**-149 (2010).
[2] G.J. Hill, et al., "VIRUS: a massively replicated 33k fiber integral field spectrograph for the upgraded Hobby-Eberly Telescope," Proc. SPIE, **7735**-21 (2010).
[3] Hill, G. J., Nicklas, H., MacQueen, P. J., Tejada de V., C., Cobos D., F. J., and Mitsch, W., "The Hobby-Eberly Telescope Low Resolution Spectrograph", in *Optical Astronomical Instrumentation*, S. D'Odorico, Ed., Proc. SPIE 3**355**, 375 (1998).
[4] Frieman, J.A., et al., "The Sloan Digital Sky Survey-II Supernova Survey: Technical Summary," Astronomical Journal, **135**, 338 (2008).
[5] Zheng et al., "First-Year Spectroscopy for the Sloan Digital Sky Survey-II Supernova Survey," Astronomical Journal, **135**, 1766 (2008).
[6] Schaefer, B.E., et al., "GRB 021004: A Massive Progenitor Star Surrounded by Shells," Astrophysical Journal, **588**, 387 (2003).
[7] Cenko, S.B., et al., "Multiwavelength Observations of GRB 050820A: An Exceptionally Energetic Event Followed from Start to Finish," Astrophysical Journal, **652**, 490 (2006).
[8] Howell, J., et al., "The Great Observatories All-sky LIRG Survey: Comparison of Ultraviolet and Far-infrared Properties," Astrophysical Journal, **715**, 572 (2010).
[9] Racusin, J.L. et al., "Broadband observations of the naked-eye γ-ray burst GRB080319B," Nature, **455**, 183 (2008).
[10] Adams, J.A., Hill, G.J., and MacQueen, P.J., "B2 0902+34: A Collapsing Protogiant Elliptical Galaxy at z = 3.4," Astrophysical Journal, **694**, 314 (2009).
[11] Schneider, D.P., et al., "Discovery of a Pair of Z=4.25 Quasars from the Sloan Digital Sky Survey," Astronomical Journal, **120**, 2183 (2000).
[12] Fan, X., et al., "A Survey of z>5.7 Quasars in the Sloan Digital Sky Survey. II. Discovery of Three Additional Quasars at z>6," Astronomical Journal, **125**, 1649 (2003).
[13] Willott, C.J., et al., "Four Quasars above Redshift 6 Discovered by the Canada-France High-z Quasar Survey," Astronomical Journal, **132**, 2435 (2007).
[14] Brandt, W.N., et al., "Observations of Faint, Hard-Band X-Ray Sources in the Field of CRSS J0030.5+2618 with the Chandra X-Ray Observatory and the Hobby-Eberly Telescope," Astronomical Journal, **119**, 2349 (2000).
[15] Brand, K., Rawlings, S., Hill, G.J., Lacy, M., Mitchell, E., & Tufts, J., "Two 100-Mpc-scale structures in the three-dimensional distribution of radio galaxies and their implications," Monthly Notice of the Royal Astronomical Society, **344**, 283 (2003).
[16] Hill, G.J., and Rawlings, S., "The TOOT survey: status and early results," New Astronomy Reviews, **47**, 373 (2003).
[17] Kirkpatrick, J. D., Henry, T. J., & McCarthy, D. W., "A standard stellar spectral sequence in the red/near-infrared - Classes K5 to M9," Astrophysical Journal Supplement, **77**, 417 (1991).
[18] Kirkpatrick, J. D., et al., "Dwarfs Cooler than ``M'': The Definition of Spectral Type ``L'' Using Discoveries from the 2 Micron All-Sky Survey (2MASS)," Astrophysical Journal, **519**, 802 (1999).
[19] Mohanty, S., Jayawardhana, R., & Basri, G., "The T Tauri Phase Down to Nearly Planetary Masses: Echelle Spectra of 82 Very Low Mass Stars and Brown Dwarfs," Astrophysical Journal, **626**, 498 (2005).
[20] Muzerolle, J., Luhman, K. L., Briceno, C., Hartmann, L., & Calvet, N., "Measuring Accretion in Young Substellar Objects: Approaching the Planetary Mass Regime," Astrophysical Journal, **625**, 906 (2005).
[21] Cruz, K. L., et al., "Meeting the Cool Neighbors. IX. The Luminosity Function of M7-L8 Ultracool Dwarfs in the Field," Astronomical Journal, **133**, 439 (2007).
[22] Luhman, K. L., "The Spatial Distribution of Brown Dwarfs in Taurus," Astrophysical Journal, **645**, 676 (2006).
[23] Luhman, K. L., et al., "A Survey for New Members of Taurus with the Spitzer Space Telescope," Astrophysical Journal, **647**,

1180 (2006).
[24] Luhman, K. L., et al., "The Disk Population of the Chamaeleon I Star-forming Region," Astrophysical Journal, **675**, 1375 (2008)
[25] Luhman, K. L., et al., "An Infrared/X-Ray Survey for New Members of the Taurus Star-Forming Region," Astrophysical Journal, **703**, 399 (2009).
[26] Hill, G.J., MacQueen, P.J., Smith, M.P., Tufts, J.R., Roth, M.M., Kelz, A., Adams, J.J., Drory, N., et al., "Design, construction, and performance of VIRUS-P: the prototype of a highly replicated integral-field spectrograph for HET," Proc. SPIE, **7014,** 257 (2008).
[27] Hill, G.J., MacQueen, P.J., Palunas, P., Barnes, S.I., & Shetrone, M.D., "Present and future instrumentation for the Hobby-Eberly Telescope," Proc. SPIE, **7014**, 5 (2008).
[28] Hwang, S. et al., 2010 in preparation
[29] Diehl, T. et al., "Characterization of DECam focal plane detectors," Proc. SPIE, **7021**, 07 (2008).
[30] Allington-Smith, J.R. et. al., "Integral Field Spectroscopy with the Gemini Multiobject Spectrograph. I. Design, Construction, and Testing," PASP, **114**, 892 (2002).
[31] Kelz, A., et al., "Prototype development of the integral-field unit for VIRUS," Proc. SPIE, **6273**, 121 (2006).
[32] M.P. Smith, G.T. Mulholland, J.A. Booth, J.M. Good, G.J. Hill, P.J. MacQueen, M.D. Rafal, R.D. Savage, B.L. Vattiat, "The cryogenic system for the VIRUS array of spectrographs on the Hobby Eberly Telescope", Proc. SPIE, **7018**,117 (2008)
[33] H. Lee, et al., "VIRUS optical tolerance and production," Proc. SPIE, **7735**-140 (2010)
[34] https://hetdex.org/
[35] http://www2.keck.hawaii.edu/inst/deimos/
[36] http://www.eso.org/sci/facilities/paranal/instruments/vimos/
[37] http://muse.univ-lyon1.fr/spip.php?article156
[38] J.L. Marshall, et al., "Production-line assembly of 150+ VIRUS spectrographs," Proc. SPIE, 7735-163 (2010).